

TASEC-Lab: A COTS-based CubeSat-like university experiment for characterizing the convective heat transfer in stratospheric balloon missions.

David González-Bárcena, Lilian Peinado-Pérez, Alejandro Fernández-Soler, Ángel Grover Pérez-Muñoz, Jose Miguel Álvarez-Romero, Fernando Ayape, Jonathan Martín, Juan Bermejo-Ballesteros, Ángel Luis Porrás-Hermoso, Daniel Alfonso-Corcuera, Sergio Marín-Coca, Manú Soto-Aranaz, Blanca Boado-Cuartero, Rafael Garcia-Romero, Santiago Pindado, Javier Pérez-Álvarez, Juan Zamorano, Ignacio Torralbo, Javier Piqueras, Isabel Pérez-Grande, Ángel Sanz-Andrés*

Universidad Politécnica de Madrid, Spain

** Corresponding author. E-mail address: david.gonzalez@upm.es.*

Abstract

The Thermal Analysis Support and Environment Characterization Laboratory (TASEC-Lab) is an experiment designed, integrated, and tested in the Universidad Politécnica de Madrid by bachelor's, master's and doctoral students. The aim of this project is to study the convection heat transfer, the thermal environment and the balloon dynamics during the ascent and float phases of a stratospheric balloon launched from the León (Spain) airfield on 16th, July 2021. TASEC-Lab has been designed following the CubeSat philosophy using commercial off-the-shelf (COTS) components. It consists of an aluminium structure of 130 x 130 x 330 mm³ with three compartments where the Electrical Power Subsystem, the Electronics, and the Heat Transfer Laboratory, are located. In addition, it carries a cup anemometer to be tested at the low-pressure conditions at high altitude to provide the relative speed of the balloon-gondola system in order to characterize the dynamics and the forced convection heat transfer. In this paper, the TASEC-Lab design is detailed as well as the different development phases considered in a university environment where all tasks were carried out by students, with the technical support of the research staff of the Instituto Universitario de Microgravedad "Ignacio da Riva" (IDR) and the group of Sistemas de Tiempo Real y Arquitectura de Servicios Telemáticos (STRAST).

Keywords

CubeSat, stratosphere, ballooning, project-based learning, convection, heat transfer.

Nomenclature

ABS	Acrylonitrile Butadiene Styrene.
AIT	Assembly Integration and Test.
APDS	Attitude and Positioning Determination Subsystem.
BEXUS	Balloon Experiments for University Students.
CAD	Computer-Aided Design.
CFRP	Carbon Fiber-Reinforced Polymer.
CNC	Computer Numerical Control.
COC	Cold Operational Case.
COTS	Commercial Off-The-Shelf.
CVCM	Collected Volatile Condensable Materials.
DC	Direct Current.

ECSS	European Cooperation for Space Standardization.
EPS	Electrical Power Subsystem.
ESA	European Space Agency.
ETSIAE	Escuela Técnica y Superior de Ingeniería Aeronáutica y del Espacio.
GMM	Geometrical Mathematical Model.
GPS	Global Positioning System.
GUI	Graphical User Interface.
HAT	Hardware Attached on Top.
HOC	Hot Operational Case.
HTL	Heat Transfer Lab.
IDR	Instituto Universitario de Microgravedad Ignacio da Riva.
IIC	Inter-Integrated Circuit.
IMU	Inertial Measurement Unit.
IoT	Internet of Things.
LAC	Laboratory of Anemometer Calibration.
LEO	Low Earth Orbit.
MUSE	Master Universitario en Sistemas Espaciales.
OBC	On-Board Computer.
OBDH	On-Board Data Handling.
OBSW	On-Board SoftWare.
SLI	Single Layer Insulation.
SPI	Serial Peripheral Interface.
STRAST	Sistemas de Tiempo Real y Arquitectura de Servicios Telemáticos.
TASEC	Thermal Analysis Support and Environment Characterization.
TASTE	The Assert Set of Tools for Engineering.
TBT	Thermal Balance Test.
TML	Total Mass Loss.
UART	Universal Asynchronous Receiver Transmitter.
UAX	Universidad Alfonso X el Sabio.
UML	Unified Modeling Language
UPM	Universidad Politécnica de Madrid.
VDA	Vapor Deposited Aluminum.

1 Introduction

During the last few years, the number of stratospheric balloon missions has increased due to the advantages they provide to the scientific community. On one hand, they are a cheaper alternative to low orbit launches and, sometimes, the scientific requirements are accomplished in both cases [1]. On the other hand, a high-altitude flight in high latitudes during the local summer period has unique characteristics with 24 hours of solar view above 99% of the atmospheric mass, which makes this type of platform suitable for studying the Sun [2]. In addition, an increasing interest in using these platforms for instrument testing has extended the launch offer to the private industry [3].

This increasing interest in using stratospheric balloons for doing science and testing space instrumentation has made the design process more complex in the course of time. For that reason, the analysis and testing processes should be more detailed to guarantee the success of the mission. The thermal behaviour of stratospheric balloon payloads is usually analysed following space systems procedures. This is because the near vacuum environment at around 40 km is very similar to that of space where radiation is the most important heat transfer mechanism [4]. However, there

are some differences that should be considered for meeting the thermal requirements of the instrumentation on board. Otherwise, the system may be oversized, or the temperature limits may be exceeded.

The main difference concerns the thermal environment. When a Low Earth Orbit (LEO) space system is analysed, orbital average values of the thermal environment are usually considered due to the characteristic times of the instrumentation. In other words, the instrumentation thermal inertia makes the short period variations of the thermal environment negligible in terms of temperature response. However, in stratospheric balloon missions the balloon has a residence time passing over a certain area longer than a LEO satellite (a period of some 90 minutes), which means they follow a quasi-steady state during the whole flight [5]. In addition, these types of flights are limited to a certain area, so only the local characteristics should be considered for characterizing the thermal environment [6].

Another difference is that found in the convective heat transfer, which is negligible in space but not in the stratosphere. In most cases, at the floating altitude, considering that the radiative heat dissipation is much larger than the convective one, it is an approach that allows the thermal engineer to analyse the system with the same tools that are employed for space systems. Nevertheless, there are some parts where the conductive or the radiative heat transfer is not as large as the convective one. The lower the pressure, the lower the natural convective heat transfer. However, in the stratosphere (~ 300 Pa), the convective regime (still in the continuous flow regime) may provide a non-negligible heat flux between close parts, depending on the characteristic lengths and thermo-optical and thermo-physical properties [7].

A completely different situation occurs during the ascent phase. Forced convection should be considered when analysing this phase. The low temperatures to be found in the tropopause (~ 11 km) together with the relative wind speed caused by the accelerations in the balloon-gondola systems make this phase a critical one in terms of the thermal control subsystem. In some cases, the minimum or maximum non-operational temperatures may be found in this phase. As is explained in Ref [8], a complete analysis with dedicated software is required to ensure survival at these extreme temperatures and to propose some solutions as pointed out in Ref [9].

The main objective of the TASEC-Lab experiment is to clarify some of the uncertainties that appear when modelling and analysing a stratospheric balloon payload from a thermal point of view. The experience acquired by the IDR thermal team during the SUNRISE I, II, and III missions [10] where they were responsible for the thermal analysis [11], has led to several research lines in this field. Being responsible for the Space Systems master's degree (MUSE) at the Universidad Politécnica de Madrid (UPM) [12], they have proposed a low-cost experiment with two parallel objectives. The technical one, which has already been explained, and an educational one, providing students from different levels with a deep experience in the development of a real project following the same phases as those in the design of a space system. For that reason, the work started with a preliminary design, which was developed into a detailed design in two months by a multidisciplinary team formed by students. Next, the assembly, integration, and tests of the different subsystems were carried out in the IDR facilities with the technical support of some professors and research staff of the IDR and STRAST research groups. In total, the development of the project lasted 5 months allowing the students to participate in it as part of their bachelor's and master's final thesis requirements.

As pointed out before, due to the limited cost budget available and the short development period, it was decided to base the design on the use of COTS components, a strategy that has been tested successfully in the stratospheric environment. 3D printed polymers components have been used instead of others since the pressure level that is reached by this mission does not produce a considerable level of outgassing. The structure, made of standard aluminium profiles follows the

CubeSat philosophy providing the students with a real-life envelope. The on-board computer (OBC) is a Raspberry Pi Model 3B+ [13] and all the electronics employed are chosen between compatible modules. The main experiment, the Heat Transfer Lab, which is located inside the main structure is a heated plate placed inside an enclosure with four openings to space allowing for an air exchange with the environment.

The design of this experiment aims at simulating real equipment onboard a scientific mission, which is usually located in non-pressurized spaces, and they dissipate power during the flight. In order to characterize the convective heat transfer, both, conduction and radiation heat exchange have been minimized by reducing the conductive coupling and the infrared emissivity of the heated plate. The temperature of the experiment is monitored in several locations by PT1000 and TC74 digital thermistors. In addition, TASEC-Lab carries two more experiments. The Attitude Determination Laboratory, which consists of an inertial measurement unit (IMU) and a global positioning system (GPS) sensor, and the Environmental Lab, which carries some sensors, such as pressure and temperature to characterize the thermal environment. Finally, a cup anemometer is also included to test their performance at low pressure in the stratosphere based on an open research line of the IDR [14]. Their results during the flight would help to characterize the flight dynamics as well as the forced convection over the experiment.

After the design, manufacturing, integration, and test activities that were developed by the students, the launch campaign provided them with a complete experience of a real project. The flight was operated by the company B2Space, as part of their program “Fly your CubeSat” which is aimed at universities [15]. The mentioned program engages universities worldwide to design, build and fly their CubeSat to the edge of space in a stratospheric flight at around 30 km of altitude. TASEC-Lab was launched sharing the same platform with an experiment from the Universidad Alfonso X el Sabio, from the León airfield, Spain, on the 16th of July 2021 at 7:30 a.m. The flight lasted 3 hours and after the balloon was pricked, the experiment was successfully retrieved, and all the data were analysed by the students. The overall results of the experiment will be discussed in a future paper where the scientific goal and the details of the Heat Transfer Lab will be drawn. Preliminary analysis as well as pre-flight test are described in Ref. [7].

Finally, it should be noted that TASEC-Lab was a prototype of an experiment selected by the European Space Agency (ESA) for the participation in the 32nd edition of the Balloon Experiments for University Students (BEXUS) programme. HERCCULES [16], which is the name of the proposed experiment, will carry a Heat Transfer Lab with additional configurations as well as radiative sensors and a differential pressure anemometer to overcome the detected limitation of cup anemometers. Its launch is expected to be performed in October 2022.

2 Working methodology

One of the main objectives of building a CubeSat-type experiment in a university environment is to provide the students with a real project experience. For that reason, on a reduced scale, this project was planned to follow the European Cooperation for Space Standardization (ECSS) phases [17] which are followed in the space system development. The activities carried out in each of these phases are described as follows:

- Phase A. Feasibility: The capabilities of the proposed system to satisfy the scientific requirements were evaluated for a stratospheric balloon mission with the technical characteristics proposed by the B2Space program. In this phase, a prototype of the main

experiment was studied and the capabilities of the OBC were evaluated to determine if the technical requirements would be attainable within the established deadlines.

- Phase B. Preliminary design: The requirements of the experiments were analysed and allocated to the subsystems, a first equipment distribution was established, the different electronics components were selected and the structure was dimensioned based on standardized aluminium profiles. The thermal environment characterization was evaluated using a preliminary thermal model.
- Phase C. Detailed design: During this phase, some of the main components were acquired and tested. The electronics scheme and the mechanical distribution were defined. A CAD (computer-aided design) model of the structure and the cup anemometer was developed. The thermal modelling and analysis were performed to propose different solutions for meeting the requirements. A power budget was established in order to define the electrical power subsystem (EPS) requirements and the dimensioning of the required battery.
- Phase D. Qualification and production: As most of the electronic components were already acquired, the production was limited to some mechanized parts of the structure and some components and mechanical supports that were manufactured using a 3D printing and CNC (computer numerical control) machines. In this phase the assembly of the electronics was developed previously to the integration process. After the CAD wiring and the procedure were defined, the integration of the experiment was developed in the IDR facilities. A preliminary functional test was performed for ensuring the correct connection of every subsystem. Once integrated, the experiment was tested at different levels as it will be explained.
- Phase E. Utilization: In this phase, the launch and the operational phase of the flight are included. The experiment was completely autonomous, so the tracking was developed by B2Space technical staff. After the flight, all recovered data was analysed.

Due to the short development period, the tasks were progressing in parallel as much as possible. Weekly meetings were carried out in order to guarantee the necessary information exchange between all the groups involved. The main activities performed during the project development are summarized in Table 1.

Table 1. Activities performed in the TASECLab development in the ECSS phases.

	Phase A	Phase B	Phase C	Phase D	Phase E
	Feasibility	Preliminary design	Detailed design	Qualification & Production	Utilization
Viability study	■				
Prototype study	■				
Requirements definition		■			
Components selection		■			
Mechanical I/F design		■			
CAD development		■			
Thermal modelling		■			
Software design		■			
Components acquisition		■			
EPS definition			■		
Electronics assembly			■		
Manufacturing			■		
Integration				■	
Tests				■	
Launch preparation				■	
Data analysis					■

Satellites are usually complex systems that require a multidisciplinary team. The huge number of tasks involved also requires the division into work packages that are carried out by different sub-teams working in parallel for the same project. For that reason, TASEC-Lab was divided into different subsystem with different responsibilities. The organization structure, where all the subsystems including the payload are assigned to student teams, is shown in Figure 1. Payload team are in charge not only of the design but also of the analysis of the experiment since they form the scientific team together with the project manager. In addition, a technical support group mainly integrated by professors, teachers and research staff of different disciplines have participated in the project.

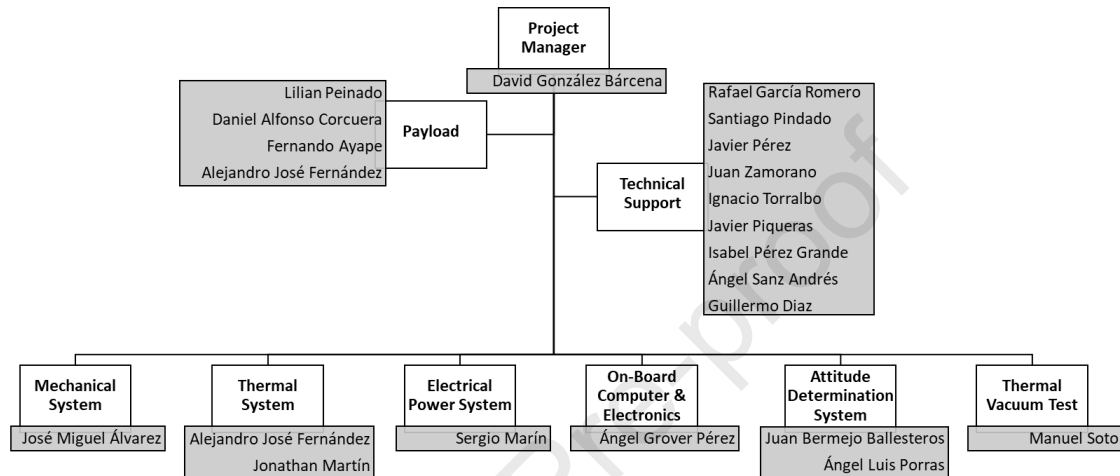


Figure 1. Organization structure of the TASEC-Lab working team.

3 TASEC-Lab Design

TASEC-Lab, which is shown in Figure 2, is an instrument that holds several experiments focused on characterizing the convective heat transfer in stratospheric balloon missions. Although most long duration balloon (LDB) flights operate above 30 km, the selected program offers a flight of 3 to 8 hours between 18 and 30 km with a goal altitude of 25 km. This allows for the characterization of thermal behaviour during the ascent phase passing through the tropopause as well as for considering the particularities of the floating phase where air temperatures are expected to be lower than -30°C .

To do so, the instrument has been divided in three parts with different objectives:

- Attitude Determination Lab: Its main objective is to characterize the flight dynamics of the balloon-gondola system (inclination and orientation) as well as the positioning, gathering data to compare with the predictive models. To do so, an IMU and a GPS sensor are carried onboard.
- Environmental Lab: In order to characterize the convective heat transfer during the flight, several parameters need to be recorded. Two pressure sensors and some thermistors are included. In addition, the relative wind velocity is measured by using a cup anemometer.
- Heat Transfer Lab: This is the main experiment of TASEC-Lab consisting of a $25 \times 50 \text{ mm}^2$ sides and 1 mm thick flat heated plate placed inside a $130 \times 130 \times 146 \text{ mm}^3$ parallelepiped volume opened to the outer ambient through four gaps with a total area of 10 cm^2 . In order to correlate the experimental data with the thermal model results, the

temperature at several points is monitored during the whole flight when different power dissipations are applied to the flat plate.

There are several reasons justifying the need for characterizing experimental heat transfer by gathering data in flight and not only in a thermal vacuum chamber. Even though a thermal test could be developed in a thermal vacuum chamber to characterize the heat transfer supporting the design, differences with respect to the real flight are expected due to the mass transfer between the cold air outside the experiment and the air inside through the abovementioned gaps. This mass transfers cannot be simulated in a thermal vacuum test unless the temperature of the air is independently controlled from the radiative interfaces and because the intrinsic motion in the real flight cannot be reproduced in a chamber at rest. Differences between the tests and the flight would provide information for which additional parameters should be considered. In addition, its behaviour during the ascent phase cannot be reproduced on the ground due to the huge number of variable parameters.

3.1 Structure and Mechanical Design

The entire subsystem corresponding to the structure was defined to simulate the CubeSat philosophy, although with differences in certain specifications. Specifically, weight restrictions were maintained (for a 3-unit CubeSat), mainly due to balloon requirements. Thus, the main external structure consists of a square prism of 130 mm x 130 mm sides and 330 mm in height. It is made of aluminium beams and closed by 1 mm thick aluminium panels, as shown in Figure 2.



Figure 2. TASEC-Lab structural configuration.

Internally, the structure is divided into three sections, separated by two aluminium trays. The components for the electrical power subsystem have been included in the lower tray (tray A). Electronics (on-board computer, IMU, pressure sensors, etc.) have been included in the middle tray (tray B). Finally, the upper compartment includes the components corresponding to the Heat Transfer Lab (tray C).

The design of the TASEC-Lab structure and configuration was carried out by the development of a detailed CAD model, which includes the structure, all the components and their interfaces. The harness and the electrical routing was also designed and integrated in the CAD model, in order to define the total space available inside the satellite.

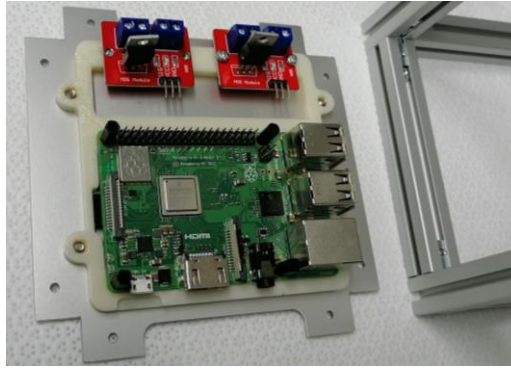


Figure 3. ABS support for attaching electronics to the tray B.

For the OBC assembly and all its compatible components, different supports have been designed and manufactured to allow them to be properly attached to the structure as shown in Figure 3. The supports have been manufactured either by 3D printer (in acrylonitrile butadiene styrene, ABS), or by mechanical milling (in delrin), depending on the mechanical and thermal specifications.

Even though the outgassing level of ABS ($TML \leq 1.13 \%$, $CVCM \leq 0.16 \%$) is outside the requirements, the pressure level that is reached by this mission and its duration make it possible the use of this material. In contrast, Delrin ($TML \leq 0.39 \%$, $CVCM \leq 0.02 \%$) is a commonly used material in space applications but more expensive that requires to be machined. Aluminum 5051 has been used for the outer panels and trays.

3.2 Heat Transfer Laboratory

The Heat Transfer Laboratory (HTL) was designed for performing thermal experiments to characterize the heat exchange due to free convection. The final dimensioning and design of the HTL is a result of on-ground tests with different prototypes, varying dimensions, heat power, heating method and supports. It consists of an aluminium flat horizontal plate of dimensions $25 \times 50 \text{ mm}^2$ and 1 mm thick with a flat heater glued to one side. The heated plate is supported by a structure made up of Delrin, which has a low thermal conductivity. These parts are shown in Figure 4 before integration. Two temperature sensors PT1000 are placed at each side of the heated plate. The temperature sensors and the heater are covered with aluminium tape to get low infrared emissivity in the whole heated plate. In order to maximize the convection heat exchange, both structural supports and surface finishing are designed to minimize the conduction and radiation heat transfer. This assembly is attached to the experiment tray in the upper enclosure where the free convection over the heated plate should take place. Atmospheric air is allowed to fill the HTL enclosure by means of small gaps made on the upper closing plate of the experiment.

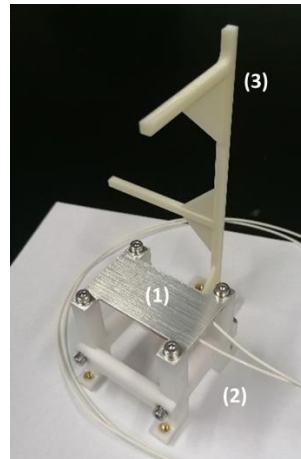


Figure 4. Heated plate (1), Delrin support (2) and ABS support structure (3) before the integration.

It is necessary to measure the atmospheric pressure and temperatures at different places during the experiment in order to characterize the heat exchange of the HTL. For this reason, the air below and above the heated plate is measured by PT1000 temperature sensors as well as the air temperature horizontally away from the heated plate and in one of the upper gaps. The measurement of air temperatures on different locations of the HTL enclosure is possible by routing the PT1000 sensors through a thin ABS support structure, as shown in Figure 4. The inner surface temperature of the lateral panels and the upper closing plate is measured with 5 TC74 temperature sensors.

The HTL is intended to operate in different power modes depending upon the phase of the flight, ascent or float, where the thermal scenarios are different. During the ascent phase, thermal transient states in the HTL are expected due to the progressive change in atmospheric pressure and temperature up to reaching the float altitude. During the operating modes for the ascent phase a fixed value of heat power is provided to the plate according to the pressure level and the mission time. During the float phase, the operating mode adjusts the heat power supplied to the plate in order to get a thermal steady state in the HTL. Operating modes in both phases, ascent and float, are designed to ensure a safe performance in terms of temperature limits, therefore, in the event of exceeding the temperature limits the heater of the plate is switched off until reaching safe temperatures again.

The different operating modes from the ascent phase and float phase until the end of the mission are performed in a sequenced and autonomous way. The HTL has carried out the experiments in the abovementioned operating modes until the end of the mission, characterized by the increase of the pressure experienced in the descent.

3.3 Cup anemometer

The TASEC-Lab is equipped with a cup anemometer for measuring the relative wind speed. This technology was chosen due to the technical problems presented by other types of anemometers (Sonic anemometers) when measuring the wind speed at high altitudes because of the low air density. The development of this solution for wind speed measuring was possible thanks to the vast experience of the IDR/UPM in studying the performance of this instrument [18–32]. The wind speed data recorded in the TASEC-Lab flight is extracted after the flight and is processed with information from:

- The ground speed of the balloon (obtained with GPS data).
- The oscillations of the nacelle containing the TASEC-Lab.

Previous to the design of TASEC-Lab, the IDR/UPM Institute had conducted research on the possibility to use the cup anemometer for measuring the wind in high altitude aerostatic balloons. This work consisted in experimental research in order to find the optimum cup size for high altitude operations. The test campaign was carried out at low speeds taking the square root of the dynamic pressure as the control parameter [14]. After the test campaign and, taking into account the results obtained, a rotor was designed to be used with a Vector Instruments A100 L2 anemometer body.

3.4 Electronics

As mentioned before, the TASEC-Lab experiment was built with COTS hardware components. In this section, the discussion is focused on the description of the OBC characteristics, sensors, and actuators of the system.

3.4.1 On-board computer

On the basis of the system requirements and taking into consideration that the environmental conditions (radiation levels, temperature, pressure, etc.) of the mission are not extreme, the OBC chosen for this mission was a Raspberry Pi (RPi) Model 3B+. It is a single board computer that is widely used in IoT (Internet of Things) projects, Industry 4.0, and embedded systems. In fact, previous stratospheric balloon missions from the BEXUS programme have used a Raspberry Pi as their main OBC [33,34]. This particular model of RPi has the following characteristics:

- Cortex-A53 Dual-core processor (ARMv8) 64-bit SoC (System on Chip) @ 1.4GHz.
- 1 GB LPDDR2 SDRAM.
- One RJ45 gigabit ethernet port.
- 40-GPIO (general-purpose input/output) header, 26 GPIO digital pins.

In addition to the input/output functions of the GPIO pins (3.3 Volts for high level), the RPi supports the following communication protocols:

- One IIC (inter-integrated circuit) interface.
- Two SPI (serial peripheral interface).
- Two UART (universal asynchronous receiver transmitter), only one is available through its GPIO pins.

3.4.2 Sensors and actuators

TASEC-Lab has three laboratories that contains a series of sensors and actuators connected to and controlled by the OBC. A context diagram of the system that presents the OBC-laboratories relationship, as well as the equipment used in each laboratory, is shown in Figure 5.

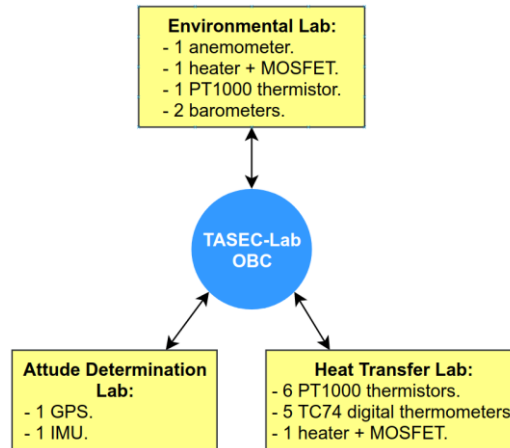


Figure 5. Context diagram of TASEC-Lab.

The equipment and the connections between them and the OBC are described in more detail in Table 2. The first column describe the device, the second column shows the number of devices included in the experiment, and the last one indicates the type of interconnection.

Table 2. Electronic equipment on board and connection interface with the OBC.

Equipment	Quantity	Interface
Grove 8-channel ADC	1	IIC
IIC MUX pHAT	1	IIC
IMU 9DOF click Mikrobús	1	IIC
TC74 digital thermistor	5	IIC ¹
IRF520 MOSFET driver module	2	GPIO
Anemometer A100L2	1	GPIO
Pressure sensor MS5611-01BA03	2	SPI
MIKROE-1032 GPS (u-blox LEA-6s)	1	USB
PT1000 thermistor	7	ADC
Silicone heater	2	MOSFET

¹The TC74 thermistors are connected through the *IIC MUX pHAT*.

Much of the equipment shown in Table 2 was assembled on the OBC through a prototyping HAT (hardware attached on top) that is attached on top of the RPi, resulting in a robust and affordable design. The prototyping HAT with the IMU, a GPS sensor, two pressure sensors and some resistors used as voltage dividers for the anemometer and PT1000 thermistors, is shown in Figure 6.



Figure 6. Prototyping HAT used for the equipment and OBC interconnections.

3.5 Software

In the following section, a brief description of the software architecture that implements the on-board data handling (OBDH) subsystem of TASEC-Lab is provided. In general, the on-board software (OBSW) of the TASEC-Lab system has to implement the following functions:

- Payload instruments operations, i.e., control of the sensors and actuators.
- Thermal control for the anemometer (a thermostat).
- Implementation of the three experiments (Heat Transfer Lab, Attitude Determination Lab, and Environmental Lab).
- On-board storage of the data acquired by the experiments.

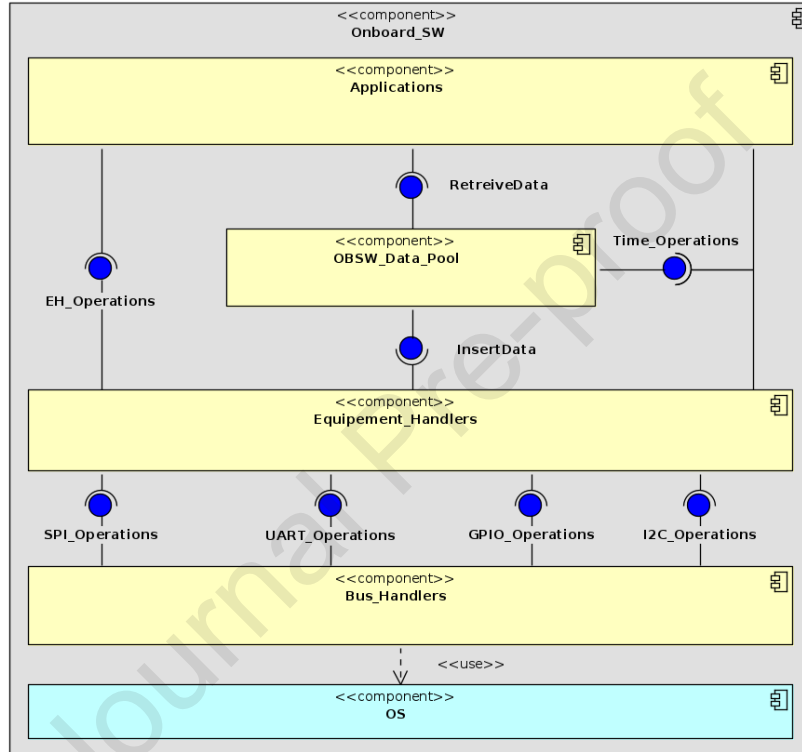


Figure 7. Software architecture of TASEC-Lab.

A UML (Unified Modeling Language) component diagram of the static architecture of TASEC-Lab is illustrated in Figure 7. It follows a layered and data pool centric architecture, which is based on the principles described in [35] and [36]. Each element of the static architecture is represented as a software component and are arranged in the following layers:

1. **Bus handlers' layer:** The purpose of this layer is to provide a set of operations that eases and abstracts the access to the hardware buses of the OBC.
2. **Equipment handlers' layer:** It is responsible for the cyclic or on-request data acquisition and actuation from the system equipment (i.e., the sensors and actuators).
3. **Data pool layer:** This layer represents a software data pool or vector containing all the equipment handlers acquired data and acts as a mediator between the *Applications* and *Equipment handlers'* layers.
4. **Applications layer:** This layer is on the top of the OBSW data pool and contains the experiments, the thermostat of the anemometer, the datalogger, system handler, and watchdog components. In other words, this layer contains software components that depend on the equipment data.

In addition to these three layers, the *operating system (OS) and device drivers* constitute a layer that sits at the bottom of all the static architecture and offers its services to all the OBSW components. The Raspberry Pi OS (Debian Buster distribution) was chosen for this experiment because (i) it is the official OS for Raspberry Pis, (ii) it offers device drivers accessible to the user-space as programming libraries, and (iii) it implements the fixed-priority real-time scheduling (SCHED_FIFO).

The system software was implemented with the TASTE (the assert set of tools for engineering) [37], a toolchain developed and maintained by ESA that follows the component based software engineering and model driven development paradigms.

Regarding the programming languages, the applications layer was implemented in SDL (specification and description language) which is automatically transformed by TASTE in Ada code. The other components were implemented mainly in C and C++. The OBSW implementation is available in this GitLab repository [38].

3.6 Attitude and Positioning Determination Subsystem

The attitude and positioning determination subsystem (APDS) is responsible for providing an estimation of the system attitude, position, and velocity. Although this information is not required during the mission, it will be useful for the thermal analysis of the balloon during the ascent phase as well as for the study of the flight dynamics. The subsystem is integrated by two devices, an IMU, which incorporates a gyroscope, an accelerometer and a magnetometer, and a GPS sensor, which supplies position, altitude, and velocity.

These sensors collect measurements during the whole mission, which are later processed to obtain the attitude evolution and the trajectory. This is performed by means of a Kalman filter, an algorithm that provides an estimation of the state of the system (position, velocity, attitude, and angular velocity in this case) based on a time series of measurements. The Kalman filter uses knowledge of the deterministic and statistical properties of the system parameters and measurements to obtain optimal estimates given the information available. A scheme of the navigation algorithm is shown in Figure 8. In this scheme, a first estimation of the attitude and position is calculated using the inertial measurements. The Kalman filter using the GPS sensor data, re-estimates the vehicle state. Additionally, IMU error and biases are estimated and fed back to achieve better precision.

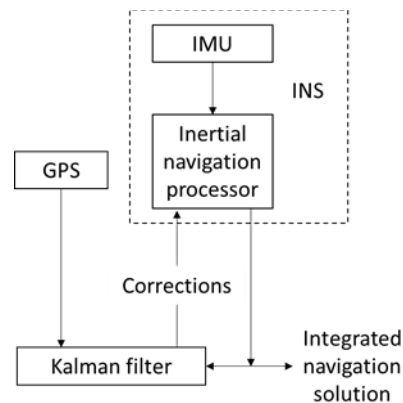


Figure 8. Navigation algorithm. The inertial processor integrates the IMU outputs to produce a navigation solution (position, velocity, and attitude). The errors estimated by the Kalman filter are fed back to correct the IMU measurements.

3.7 Electrical Power Subsystem

The electrical components of the TASEC-Lab (e.g., OBC, temperature and pressure sensors, cup anemometer, GPS sensor, heaters...) have their own voltage and power consumption requirements. Compliance with these requirements is of crucial importance to avoid malfunctions of other subsystems and ensure the success of the mission. Therefore, a good design of the Electrical Power Subsystem is required.

The EPS supplies, regulates, and distributes electric power to the rest of the TASEC-Lab subsystems. It mainly consists of a 24 V Li-ion battery, a highly efficient 5 and 12 V output voltage DC-DC switching converters, a distribution harness, and a mechanical switch. These components are shown in Figure 9.

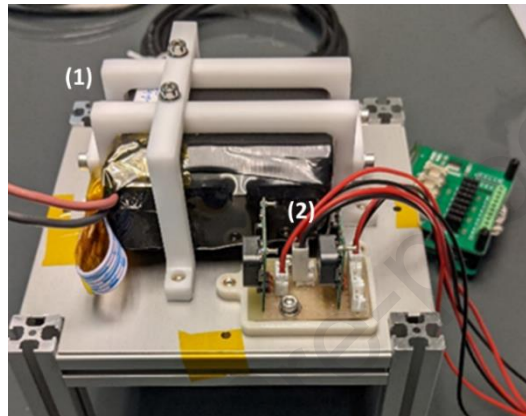


Figure 9. Integration of the TASEC-Lab EPS. Battery (1) and DC-DC converters (2).

A simplified circuit of the EPS is shown in Figure 10. With the activation of the mechanical switch, the EPS bus provides power to the DC-DC converters. The first DC-DC converter supplies power at 5 V to the OBC which, in turn, feeds other components at 3.3 and 5 V voltage. On the other hand, the second DC-DC converter provides power at 12 V voltage to the anemometer, its heater, and the experiment heater.

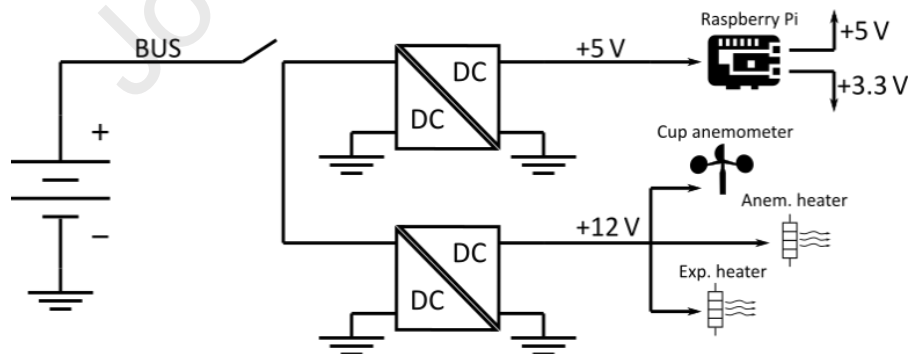


Figure 10. EPS simplified electrical circuit.

3.8 Thermal Control Subsystem

Regarding the thermal control subsystem, its purpose is to maintain the experiment and its instruments within its temperature ranges during the whole mission. The battery and the anemometer are the most critical elements from the thermal point of view. On the one hand, the battery should not operate below 5 °C. Therefore, in order to isolate it from the cool gondola, the tray where the battery is assembled is covered with vapour deposited aluminium (VDA) single layer insulation (SLI) to reduce the radiative cooling (Figure 11c). Besides, this tray is conductively decoupled from the vertical satellite beams through delrin washers. On the other

hand, the anemometer shall operate within a narrow range, between 15 °C and 25 °C with a tolerance of ± 5 °C, as the working temperature conditions should not be far from the ones in which the cup anemometer was calibrated. To achieve this, the anemometer is covered with black SLI (Figure 11b) and a heat tape is directly glued to the rotor the rotor shaft to control the temperature actively and reduce changes in bearing friction that could affect the accuracy of the wind speed measurements. Finally, the closure panels are black painted to increase the solar absorptance (Figure 11a).

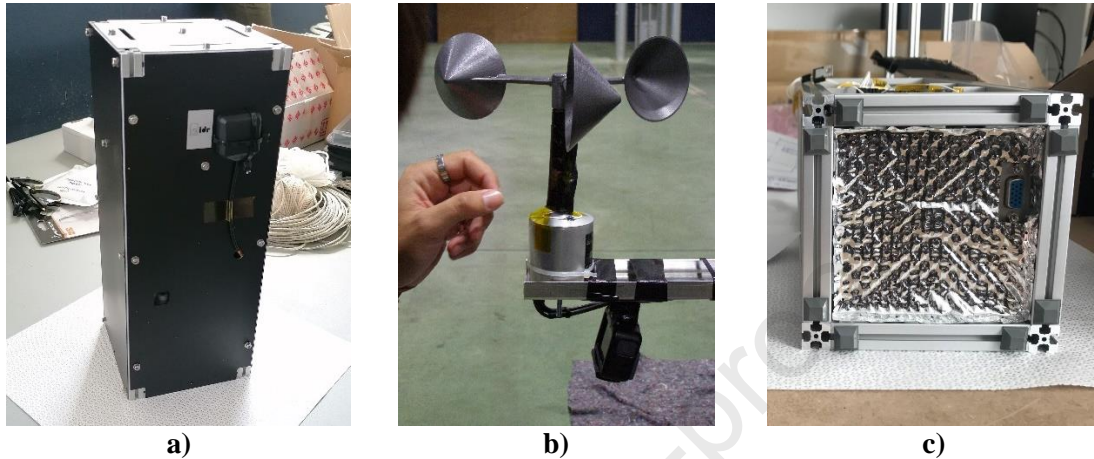


Figure 11. Passive thermal hardware of TASEC-Lab: a) black painted outer surfaces; b) anemometer black SLI; c) tray A VDA SLI:

To verify the requirements for the thermal control subsystem, the geometrical mathematical model (GMM) and the thermal mathematical model (TMM) of the satellite have been developed in ESATAN-TMS as shown in Figure 12. The thermal environment has been characterized for the location of the TASEC-Lab launch for both, the ascent and float phases [6,8]. The ascent phase has been analysed, following the methodology depicted in [39] considering two launch times, at 12 am (hot case) and at 5 am (cold case). In addition, two steady-state cases at the two potential float altitudes (18 and 30 km) have been analysed.

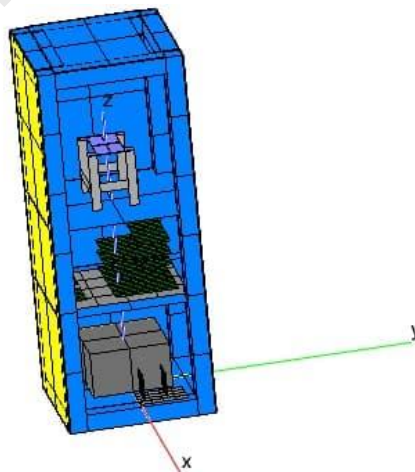


Figure 12. ESATAN-TMS GMM of the TASEC-Lab experiment.

4 Assembly, Integration and Test (AIT) activities

4.1 Integration procedure

The integration of TASEC-Lab was performed at the IDR premises by the student team according to a coherent and safe procedure, taking into account the wiring footprints. According to the mechanical design, the integration was planned to be performed sequentially by trays. First of all, the main structure was assembled. Once the lower tray, tray A, was integrated (battery, converters, and the anemometer connector), it was attached to the horizontal profiles using Delrin washers to minimize the heat conduction between the tray and the structure. Then, the electronics tray, tray B, with the mosfets and the Raspberry Pi, was also integrated using L-shaped nuts (Figure 13a). This tray allows the wiring to/from the equipment below/above by means of two lateral gaps in the edges of the tray. At this point the wires routed in the lower tray were connected to the electronics. Next, the higher plate, corresponding to the Heat Transfer Lab, tray C, was assembled and the PT1000 sensors were positioned at their respective positions. Once tray C was located in the main structure, the RPi HATs were integrated after connecting all the temperature sensors (Figure 13b).

Once these trays are fixed to the structure, it is necessary to attach the lateral panels, labelled +X, +Y, -X and -Y. This assembly starts with the +X panel, where two holes are machined to allow the ethernet connection to the Raspberry Pi and the connection for the GPS antenna, placed in the external side of +X panel. This step is followed by fixing +Y, where the GPS device is mounted on the panel (in the electronics enclosure area) and connected to the electronics and antenna. Then, the lateral panels -X and -Y are assembled. In these steps, a TC74 temperature sensor is glued to the internal side of each panel (in the HTL enclosure area) before attaching the panel to the structure.

After the assembly of the lateral panels, a TC74 is glued to the internal side of the tray D (upper tray) and then, it is mounted on the top of the structure, closing the instrument. The last step in the integration procedure is mounting the SLI on the external side of the tray A.

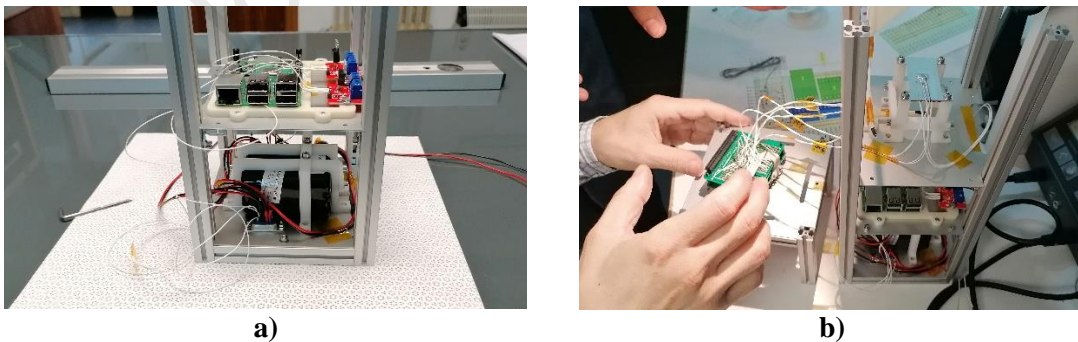


Figure 13. a) Tray B and b) electronics integration.

4.2 Software testing

The software testing of an embedded system as in the case of TASEC-Lab is quite different from other types of systems because it has to be performed on both software and hardware in order to find the defects and perform the verification and validation of the system. Then, for the unit and integration testing, a prototyping model with a breadboard was built as shown in Figure 14. This was a partial model that contained the same OBC type and at least one unit of each equipment listed in Table 2.



Figure 14. Prototyping model of TASEC-Lab used for software testing.

The verification of the *bus handlers* and *equipment handlers* layers was automated with the **gtest** tool, a unit testing library for the C++ programming language. On the other hand, to perform the verification of the other layers and the validation of the system a GUI (graphical user interface) was built. This GUI was automatically generated with the TASTE toolchain [37]. It displays all the data from the devices in real time and provides some fields to send commands to the system. The GUI of TASEC-Lab was used during the functional testing with the Attitude and Environmental Laboratory and some commands for the Heat Transfer Lab. It shown in Figure 15.

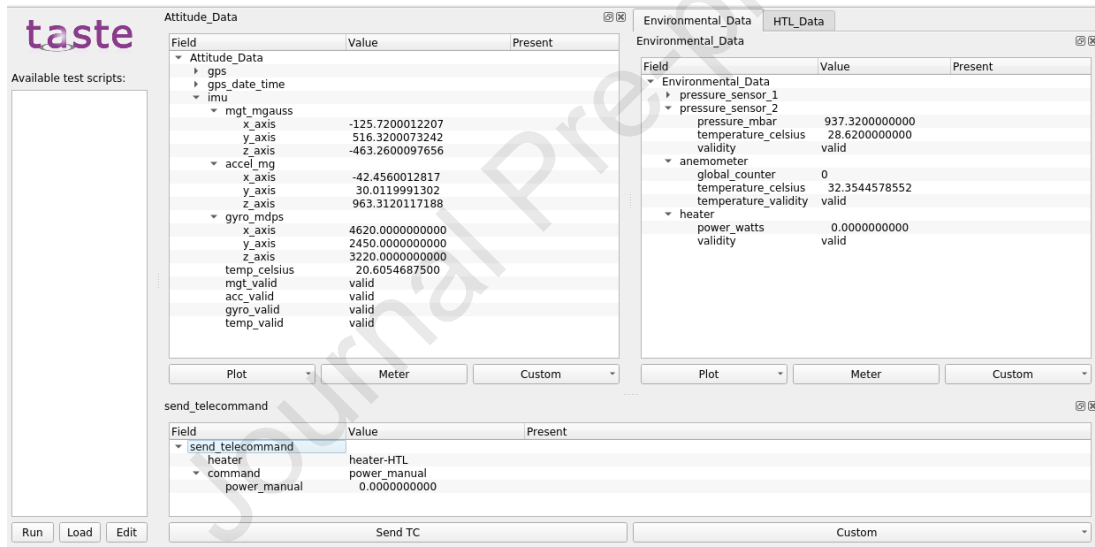


Figure 15. GUI of TASEC-Lab used during the functional testing.

4.3 Electrical Power Subsystem testing

TASEC-Lab EPS has been tested to ensure it can provide enough power to all the electrical components without exceeding safe margins of the remaining battery capacity after the mission. In the first place, a detailed power budget during the mission was established. Then, a worst-case power consumptions profile, as shown in Figure 16, was emulated with two programmable electronic loads connected to the battery, in order to measure and record its voltage. The results show that, despite the long duration of the mission, the battery voltage did not drop to critical levels, thanks to the low power consumption of the devices.

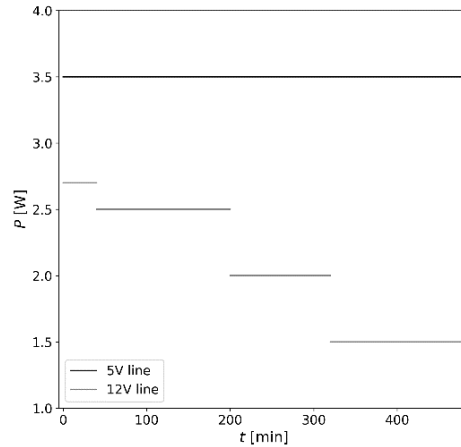


Figure 16 Variation with time t of the estimated power consumption P of the 5 V and 12 V lines.

Moreover, as TASEC-Lab (or a similar experiment platform) is expected to perform additional flights, with different power consumption requirements, the EPS has been modelled to predict its behaviour. For this purpose, the battery and the DC-DC converters were characterized performing tests and fitting analytical models to the experimental data.

An electronic load was used to carry out several battery dischargings to characterize the battery performance under the estimated flight loads. Then, an analytical battery model (based on the one developed at the IDR/UPM Institute [40]) was implemented by using the discharging test data to calibrate the model parameters. Besides, the efficiency of the DC-DC converters was calculated comparing the measured values of the input and output voltages and currents. In addition, a total of three models were used to characterize the converters [41,42]. Finally, a complete EPS model was built and validated by comparison with the experimental data as shown in Figure 17 [43].

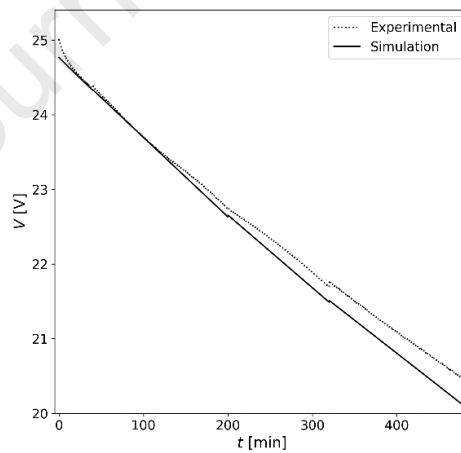


Figure 17 Evolution of the battery voltage during the test (dotted line) and the simulation (solid line).

4.4 Attitude and Positioning Determination Subsystem testing

The aim of the APDS test campaign was to ensure that it works as expected. Specifically, the following items were checked:

- Measurements are taken properly (both magnitude and direction).
- IMU data is duly send to the OBC and correctly stored.
- The state is correctly estimated by the Kalman filter.

Additionally, the measures taken in some tests will be used to assess the misalignment of the sensor axes, the error bias, and the measurement noise. The tests were divided into two categories: preliminary and functional. The former included those tests focused on checking that the IMU and the GPS sensor were operational. In particular, the directions of the IMU axes were verified and the GPS sensor functioning was checked. The second category gathered the tests aimed to verify that the IMU and GPS sensor operated correctly after the integration, to measure the misalignment of the sensor's axes and to gather data from the magnetometer for further analysis. A detailed list of the test performed is shown in Table 3.

Table 3. List of APDS tests performed.

Category	Test
Preliminary	<ul style="list-style-type: none"> • Check GPS sensor is operative. • Check IMU is operative. • Check IMU axes.
	<ul style="list-style-type: none"> • Check GPS sensor can retrieve position accurately. • Retrieve data from IMU static test for bias and noise characterization. • Retrieve data for inertial navigation algorithm testing. • Check magnetometer calibration. • Retrieve data for axis misalignment characterization.

4.5 Anemometer calibration

The anemometer body with the home-made cup rotor was calibrated at the Laboratory of Anemometer Calibration (LAC) of the IDR/UPM Institute. The calibration curve, shown in Figure 18, is the transfer function that provides the horizontal wind speed as a function of the number of pulses measured from the anemometer output. Finally, to avoid the influence of the outside air temperature, a resistor was attached to the anemometer's shaft for heating, ensuring that the working temperature was similar to the calibration temperature. This was an important issue as recent research has shown that a decrease up to 1% in the rotor turning speed can appear when working at low temperatures, caused by an increase in bearing friction [44].

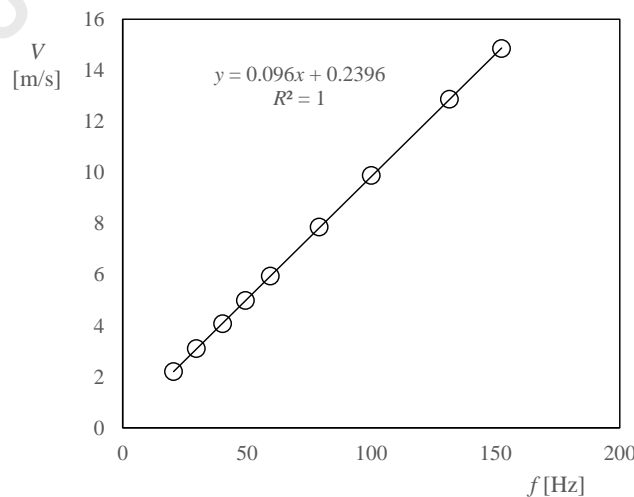


Figure 18. Transfer function (i.e., wind speed, V , vs. anemometer output frequency, f) of the TASEC-Lab cup anemometer measured at LAC-IDR/UPM.

4.6 Thermal Balance Test

A thermal balance test (TBT) was carried out at the thermal vacuum chamber of the Thermodynamics laboratory at ETSIAE/UPM (Escuela Técnica Superior de Ingeniería Aeronáutica y del Espacio premises (Figure 19). The aim of this test was to check the proper performance of the main components of TASEC-Lab under the worst-case environmental conditions at the float pressure level as well as to carry out a thermal model correlation. The maximum and minimum temperatures used as boundary conditions for the conductive interface (baseplate) and the radiative one (shroud) were obtained from the steady-state analysis performed in ESATAN-TMS. They are the result of a combination of the internal operation (heat dissipation) of the experiment and the external environment (air temperature, pressure, and radiative thermal loads).

During the float phase, depending on the variation of the thermal radiative loads and the up and down oscillating motion of the balloon, the steady state may not be reached but a quasi-steady state will. Therefore, the extreme thermal scenario for HOC is defining in steady state conditions. HOC is set at 1380 Pa (approximately the pressure at 30 km), radiative temperature of 42 °C, conductive temperature of 31 °C and 0.8 W heat power dissipated in the HTL experiment at power on. The COC parameters are set at 8400 Pa (approximately 18 km altitude), radiative temperature -3 °C, conductive temperature -10 °C and experiment power on with the HTL heater off.



Figure 19. Opened TVAC chamber with TASEC-Lab and thermocouples connections.

The measurements obtained during the test from several thermocouples placed at selected positions on the structure, as well as the internal temperature sensors, allowed us to perform the mathematical model correlation using the measured temperatures during both the hot and cold balance stages. In both cases, the battery, which has the strictest temperature requirements ($5\text{ °C} < T < 40\text{ °C}$), was used as the reference temperature point. The test profile corresponding to the external thermocouples is shown in Figure 20 where the functional tests are outlined.

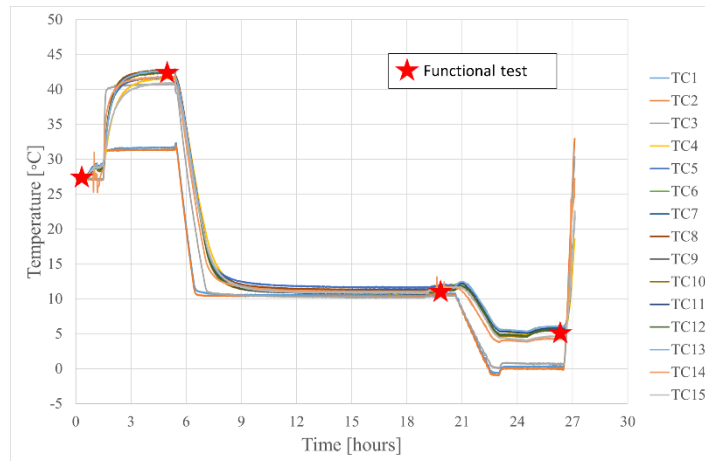


Figure 20. Variation with time of several thermocouple temperature measurements during the TBT.

4.7 Functional test

A functional test was performed in order to check the correct software performance through all operating modes. This test was carried out in the thermal vacuum chamber to apply the pressure at the required levels for the software response, but no thermal scenario was set in the functional test. All the parameters of interest measured by the instrument were monitored and recorded in the same way as the TBT.

The autonomous sequence of operating modes provided by the software was checked in terms of different events reached in pressure, time, and temperature. In order to initiate the sequences provoked by either or both the pressure and temperature events, the chamber pressure and the heat power supplied to the HTL were varied, respectively. Some responses can be triggered by multiple either separated or combined events, so the functional tests collected all the possibilities.

5 Launch campaign

The TASEC-Lab launch took place from the military airport of León, Spain, on 16th of July 2021. As pointed out before, the instrument was flown on board a gondola supplied by B2Space, which is also the company in charge of the launch operation. Once the experiment arrived at the Airport facilities, a pre-flight test was performed to check the correct performance of every element. Then, the last battery charge was conducted by the UPM students before the gondola integration.

The gondola consists of a baseplate made of CFRP (carbon fiber-reinforced polymer) with four 350 mm aluminium struts attached to a CFRP bite in the upper part. TASEC-Lab was located in a corner of the baseplate while the UAX experiment was placed in the opposite corner. The B2Space avionics as well as some cameras were also allocated in the gondola. The cup anemometer was attached to an aluminium arm in the upper part facing upwards. The final configuration is shown in Figure 21a during the parachute integration tasks.



Figure 21. a) Gondola final configuration during the parachute integration and b) balloon film during the inflation.

The gondola is attached to the balloon on the upper part through a rotatory bar which allows both systems (gondola and balloon) to rotate independently. In this case, the gondola is flown with a zero-pressure balloon made of polyethylene with 30 m^3 of helium, as shown in Figure 21b. A pyrotechnic system would be responsible for pricking the balloon, giving way to the deployment of the parachute for landing.

6 Flight and results

The launch was expected to be performed at 7:00 am, however, the high winds during the sunrise forced a delay. The TASEC-Lab program started 2 minutes before the release, which took place at 7.30 am. During approximately an hour, it was climbing up to around 18 km before the balloon was pricked. Due to military restriction the flight was shorter than expected and it was terminated during the ascent phase. However, data retrieved provided useful information for the postprocessing.

- Heat Transfer Lab:** Even though it was not possible to reach the float altitude to consider free convective heat transfer, an interesting model correlation for the ascent phase analysis was carried out accounting for the mass exchange through the open gaps on the top of the experiment. Due to the final configuration of the gondola, a direct air flux entered through these gaps providing a lower temperature than expected. The consideration of a mass exchange between the inner and outer air provides a close adjustment to the flight data as shown in Figure 22. Results of this correlation will be included in a future paper.

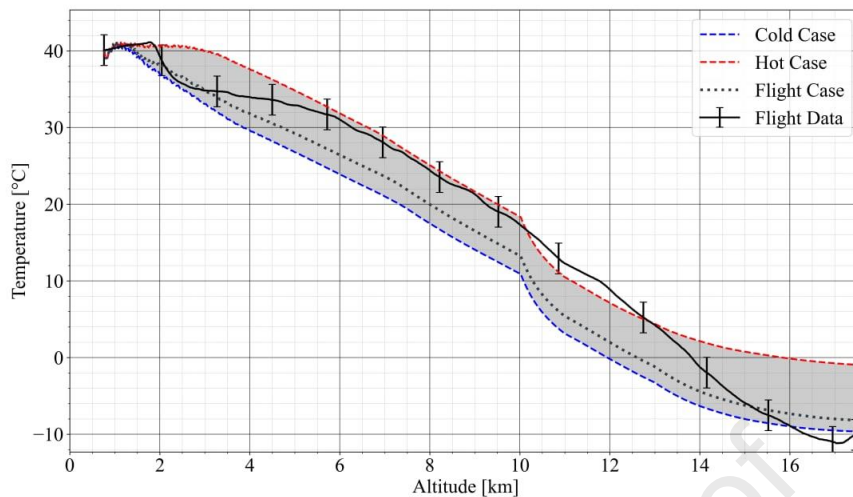


Figure 22. Predicted hot and cold worst-cases as well as flight case for the ascent phase compared to flight data.

- Attitude Determination Lab:** The relative attitude of the experiment with respect to a reference navigation frame was not possible to determine for two reasons. On the one hand, even if IMU data were retrieved successfully the post-process shows that the precision of the selected component was not enough to obtain the gondola orientation due to the accumulated error. The measurements of the GPS integrated could have helped to filter the IMU measurements and correct the bias errors. However due to a bad configuration of the GPS, the signal was lost when the balloon reached an altitude around 12000 m as shown in Figure 23. On the other hand, a problem was encountered with the magnetometer measurements, as the experiment was started without proper calibration of the magnetometers when the other equipments were activated. Without this calibration, the measured magnetic field is distorted, and the calculated attitude is poorly determined. To process the data stored during the flight, it is necessary to perform a calibration campaign of the magnetometers to obtain their calibration matrix. This would reduce the uncertainty in the calculated attitude.

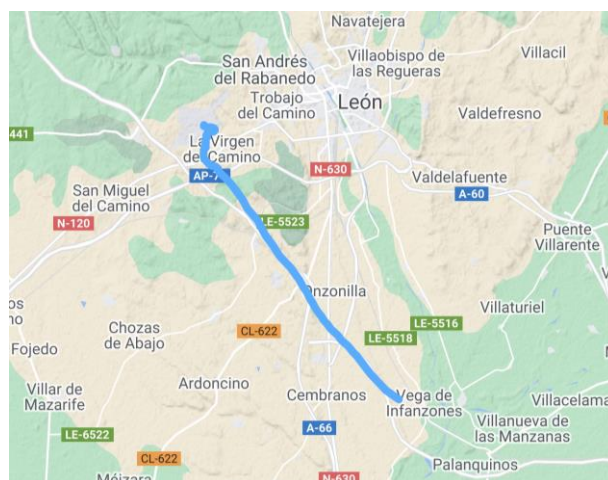


Figure 23. TASEC-Lab trajectory during the ascent phase up to 12 km.

- Environmental Lab:** Temperature and pressure sensors worked as expected as well as the anemometer that provided interesting data about the measured air speed. The

anemometer's output signal was sampled at 3 kHz rate, counting the number of pulses (that is, when the voltage level of the output signal rose above 3.3 V) per second produced by the rotation of the instrument's shaft. More information on the opto-electronic system of the anemometer that produces the pulse train output signal can be found in Refs. [22–24]. In Figure 24, the vertical speed of the lab, V_z , based on the GPS until 12000 m height, and from this point based on the height above ground calculated with the pressure measurements. Additionally, the output frequency, f , of the cup anemometer has been included in the graph from Figure 24. The results indicate a low horizontal velocity, with average values around 1 m/s, up to the tropopause. From this point, it seems that quite large wind velocities have been measured.

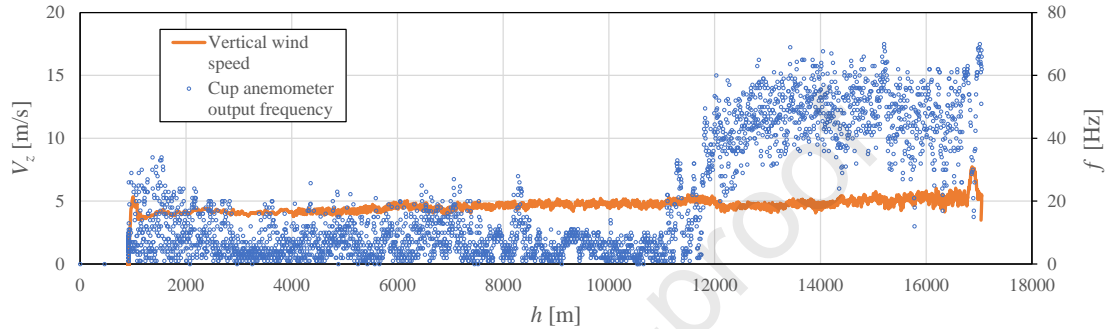


Figure 24. Vertical speed of TASEC-Lab, V_z , based on the GPS and pressure sensors (orange) and output frequency, f , from the cup anemometer.

7 Conclusions

The developed work around the TASEC-Lab project from the design to the flight has been summarized in this paper. It aims at helping other educational institutions or companies to develop a low-cost design for stratospheric flights showing the main parts of the design and the required test activities for guaranteeing the success of the mission.

This work has been performed by students from the Universidad Politécnica de Madrid, in an academic environment during a university semester. They counted on the technical support of the IDR and STRAST research staff, that is also responsible for the educational activities of the Space Systems master degree (MUSE) of the UPM. For that reason, this project has been treated as a Space project (one of the master activities) with the aim of providing the students with a real experience in the space field. In spite of the reduced period of time for the development of this instrument, the organization of this project has been a success.

The design of TASEC-Lab has kept to the CubeSat philosophy as part of the flight program offered by the company B2Space, which is responsible of the launch of the experiment. TASEC-Lab design has been based on the use of COTS components, as well as in-house manufactured elements, getting an optimum design that has worked properly during the whole flight. In addition, all tests have been performed at the IDR facilities ensuring the correct performance of the equipment before the launch.

During the launch campaign, both, the university team and the company staff worked together in establishing the interfaces between the experiment and the gondola. It was successfully launched from León airfield in Spain and it was recovered from the landing location with no damage to the structure. This will allow us to perform future launches aiming to increase the amount of

measurements taken, which could help us to improve the convective heat transfer modelling in these kind of flights.

Lessons learnt during the development of TASEC-Lab will help students in the design of the HERCCULES experiment which is going to be flown in BEXUS 32 programme in October 2022. An improved concept of an anemometer will be implemented in the experiment based on differential pressure measurements. The Heat Transfer Lab will include more configurations for characterizing the convective heat transfer. In addition, technology successfully used here such as 3D printed materials, pressure sensors, PT1000 thermistors, GPS sensor (with the correct configuration) and more, will be also used in HERCCULES.

Acknowledgments

The authors would like to acknowledge all the IDR and STRAST staff for their contribution to this project as well as the UPM Space Systems master's degree students that have participated in the design of TASEC-Lab. Project OAPES Y2020/NMT-6427 has contributed to this formative activity.

References

- [1] T. Kremic, K. Hibbitts, E. Young, R. Landis, K. Noll, K. Baines, Assessing the potential of stratospheric balloons for planetary science, in: IEEE Aerospace Conference Proceedings, 2013. <https://doi.org/10.1109/AERO.2013.6496843>.
- [2] P. Barthol, A. Gandorfer, S.K. Solanki, M. Schüssler, B. Chares, W. Curdt, W. Deutsch, A. Feller, D. Germerott, B. Grauf, others, The sunrise mission, *Solar Physics*. 268 (2011) 1–34.
- [3] S.A. Stern, J. Poynter, T. MacCallum, World view stratospheric ballooning capabilities, research, and commercial applications, in: IEEE Aerospace Conference Proceedings, 2017. <https://doi.org/10.1109/AERO.2017.7943931>.
- [4] D. González-bárcena, I. Pérez-grande, Á. Sanz-andrés, J. Piqueras-carreño, I. Torralbo, Challenges in the thermal analyses of the ascent and float phases of SUNRISE III, (2020) 1–12.
- [5] D. González-Bárcena, A. González-Llana, I. Pérez-Grande, Á. Sanz-Andrés, Parametric Worst Case thermal environment conditions selection for Polar Summer Long Duration Balloon missions, 2019.
- [6] A. González-Llana, D. González-Bárcena, I. Pérez-Grande, Á. Sanz-Andrés, Selection of extreme environmental conditions, albedo coefficient and Earth infrared radiation, for polar summer Long Duration Balloon missions, *Acta Astronautica*. 148 (2018). <https://doi.org/10.1016/j.actaastro.2018.05.016>.
- [7] L.P. Pérez, F. Ayape, J. Martín, D.G. Bárcena, V. Muntean, Experiments of the Prototype for a Stratospheric Balloon- borne Heat Transfer Experiments of the Prototype for a Stratospheric Balloon- borne Heat Transfer Laboratory, (2021) 0–12.
- [8] D. González-Bárcena, A. Fernández-Soler, I. Pérez-Grande, Á. Sanz-Andrés, Real Data-based Thermal Environment Definition for the Ascent Phase of Polar-Summer Long Duration Balloon Missions from Esrange (Sweden), *Acta Astronautica*. (2020). <https://doi.org/10.1016/j.actaastro.2020.01.024>.
- [9] I. Pérez-Grande, A. Sanz-Andrés, N. Bezdenejnykh, P. Barthol, Transient thermal analysis

- during the ascent phase of a balloon-borne payload. Comparison with SUNRISE test flight measurements, *Applied Thermal Engineering*. 29 (2009) 1507–1513.
- [10] S.K. Solanki, T.L. Riethmüller, P. Barthol, S. Danilovic, W. Deutsch, H.-P. Doerr, A. Feller, A. Gandorfer, D. Germerott, L. Gizon, others, The second flight of the SUNRISE balloon-borne solar observatory: overview of instrument updates, the flight, the data, and first results, *The Astrophysical Journal Supplement Series*. 229 (2017) 2.
- [11] I. Pérez-Grande, A. Sanz-Andrés, N. Bezdenejnykh, A. Farrahi, P. Barthol, R. Meller, Thermal control of SUNRISE, a balloon-borne solar telescope, *Proceedings of the Institution of Mechanical Engineers, Part G: Journal of Aerospace Engineering*. 225 (2011) 1037–1049.
- [12] S. Pindado, Á. Sanz, S. Franchini, I. Pérez-Grande, G. Alonso, J. Pérez, F. Sorribes-Palmer, J. Cubas, A. García, E. Roibás, A. Fernández, MUSE (Master in Space Systems), an Advanced Master 's Degree in Space Engineering, Athens: ATINER'S Conference Paper Series, No: ENGEDU2016-1953. (2016) 1–16.
- [13] www.raspberrypi.org/, Raspberry Pi 3 Model B - Raspberry Pi, Raspberry Pi 3 Model B. (2016).
- [14] Á. Ramos-Cenzano, E. López-Núñez, D. Alfonso-Corcuera, M. Ogueta-Gutiérrez, S. Pindado, On cup anemometer performance at high altitude above ground, *Flow Measurement and Instrumentation*. (2021). <https://doi.org/10.1016/j.flowmeasinst.2021.101956>.
- [15] B2Space, “Fly your CubeSat” International University Programme, (n.d.). <https://b2-space.com/blue-jay-programme/>.
- [16] J.M. Álvarez, HERCCULES. An experiment from UPM for BEXUS 32, (n.d.). <https://blogs.upm.es/herccules/>.
- [17] ECSS-M-ST-10C Rev. 1 - Space project management - Project planning and implementation, Standard, European Cooperation for Space Standardization (ECSS), Noordwijk, The Netherlands. (2009).
- [18] S. Pindado, E. Vega, A. Martínez, E. Meseguer, S. Franchini, I. Pérez, Analysis of calibration results from cup and propeller anemometers. Influence on wind turbine Annual Energy Production (AEP) calculations, *Wind Energy*. 14 (2011) 119–132. <https://doi.org/10.1002/we.407>.
- [19] S. Pindado, A. Barrero-Gil, A. Sanz, Cup Anemometers' Loss of Performance Due to Ageing Processes, and Its Effect on Annual Energy Production (AEP) Estimates, *Energies*. 5 (2012) 1664–1685. <https://doi.org/10.3390/en5051664>.
- [20] A. Martínez, E. Vega, S. Pindado, E. Meseguer, L. García, Deviations of cup anemometer rotational speed measurements due to steady state harmonic accelerations of the rotor, *Measurement*. 90 (2016) 483–490. <https://doi.org/10.1016/j.measurement.2016.05.011>.
- [21] E. Roibas-Millan, J. Cubas, S. Pindado, Studies on cup anemometer performances carried out at IDR/UPM Institute. Past and present research, *Energies*. 10 (2017) 1–17. <https://doi.org/10.3390/en10111860>.
- [22] A. Ramos-Cenzano, M. Ogueta-Gutiérrez, S. Pindado, Cup anemometer measurement errors due to problems in the output signal generator system, *Flow Measurement and Instrumentation*. 69 (2019) 101621. <https://doi.org/10.1016/j.flowmeasinst.2019.101621>.
- [23] A. Ramos-Cenzano, M. Ogueta-Gutierrez, S. Pindado, On the signature of cup anemometers' opto-electronic output signal: Extraction based on Fourier analysis, *Measurement*. 145 (2019) 495–499. <https://doi.org/10.1016/j.measurement.2019.06.001>.

- [24] A. Ramos-Cenzano, M. Ogueta-Gutierrez, S. Pindado, On the output frequency measurement within cup anemometer calibrations, *Measurement*. 136 (2019) 718–723. <https://doi.org/10.1016/j.measurement.2019.01.015>.
- [25] S. Pindado, A. Sanz, A. Wery, Deviation of Cup and Propeller Anemometer Calibration Results with Air Density, *Energies*. 5 (2012) 683–701. <https://doi.org/10.3390/en5030683>.
- [26] S. Pindado, J. Pérez, S. Avila-Sanchez, On cup anemometer rotor aerodynamics, *Sensors*. 12 (2012) 6198–6217. <https://doi.org/10.3390/s120506198>.
- [27] S. Pindado, I. Pérez, M. Aguado, Fourier analysis of the aerodynamic behavior of cup anemometers, *Measurement Science and Technology*. 24 (2013) 065802 (9 pp). <https://doi.org/10.1088/0957-0233/24/6/065802>.
- [28] S. Pindado, J. Cubas, A. Sanz-Andrés, Aerodynamic analysis of cup anemometers performance. The stationary harmonic response, *The Scientific World Journal*. 2013 (2013) 1–11. <https://doi.org/10.1155/2013/197325>.
- [29] S. Pindado, J. Cubas, F. Sorribes-Palmer, The Cup Anemometer, a Fundamental Meteorological Instrument for the Wind Energy Industry. Research at the IDR/UPM Institute, *Sensors*. 14 (2014) 21418–21452. <https://doi.org/10.3390/s141121418>.
- [30] E. Vega, S. Pindado, A. Martínez, E. Meseguer, L. García, Anomaly detection on cup anemometers, *Measurement Science and Technology*. 25 (2014) 127002 (6pp).
- [31] S. Pindado, A. Ramos-Cenzano, J. Cubas, Improved analytical method to study the cup anemometer performance, *Measurement Science and Technology*. 26 (2015) 1–6. <https://doi.org/10.1088/0957-0233/26/10/107001>.
- [32] S. Pindado, J. Cubas, F. Sorribes-Palmer, On the harmonic analysis of cup anemometer rotation speed: A principle to monitor performance and maintenance status of rotating meteorological sensors, *Measurement*. 73 (2015) 401–418. <https://doi.org/10.1016/j.measurement.2015.05.032>.
- [33] T.A. Stein, et al., Student Experiment Documentation - BEXUS 20. Cosmic Particle Telescope, 2016. http://rexbexus.net/wp-content/uploads/2016/05/BX20_CPT-SCOPE_SEDv5-0_18May16_reducedFileSize.pdf.
- [34] E.J. Martínez Pérez, Student Experiment Documentation - BEXUS 19. Attitude determination system for a pico satellite based in a star tracker, a horizon sensor and Earth's magnetic field measurements, 2015. http://rexbexus.net/wp-content/uploads/2015/07/BX19_GRANASAT_SED_v5-0_15Jan15-reduced.pdf.
- [35] J. Eickhoff, Onboard Computers, Onboard Software and Satellite Operations, 2019.
- [36] J. Zamorano, J.A. de la Puente, OBDH_LABS, (n.d.). https://github.com/STR-UPM/OBDH_LABS.
- [37] European Space Agency, TASTE: A tool-chain targeting heterogeneous embedded systems, using a model-based development approach, (n.d.). <https://taste.tools/> (accessed July 30, 2021).
- [38] Á.G. Pérez, TASEC-Lab repository, (n.d.). https://gitlab.com/AngelPerezM/TASEC-Lab_UPM.
- [39] A. Fernández-Soler, D. González-Bárcena, I. Pérez-Grande, Á. Sanz-Andrés, Thermal Analysis of SUNRISE III ascent phase, in: 50th International Conference on Environmental Systems, 2021.
- [40] A. Porrás-Hermoso, S. Pindado, J. Cubas, Lithium-ion battery performance modeling based on the energy discharge level, *Measurement Science and Technology*. (2018).

- <https://doi.org/10.1088/1361-6501/aae231>.
- [41] S. Pindado, E. Roibas-Millan, J. Cubas, J.M. Alvarez, D. Alfonso-Corcuera, J.L. Cubero-Estalrich, A. Gonzalez-Estrada, M. Sanabria-Pinzon, R. Jado-Puente, Simplified Lambert W-Function Math Equations When Applied to Photovoltaic Systems Modeling, *IEEE Transactions on Industry Applications*. (2021). <https://doi.org/10.1109/TIA.2021.3052858>.
- [42] Á. Porras-Hermoso, B. Cobo-Lopez, J. Cubas, S. Pindado, Simple solar panels/battery modeling for spacecraft power distribution systems, *Acta Astronautica*. (2021). <https://doi.org/10.1016/j.actaastro.2020.10.036>.
- [43] S. Marín-Coca, D. González-Bárcena, S. Pindado, E. Roibas-Millan, Modelling and numerical simulation of the TASEC-Lab power subsystem, in: 10th International Conference on Mathematical Modeling in Physical Sciences, 2021.
- [44] D. Alfonso-Corcuera, S. Pindado, M. Ogueta-Gutiérrez, Á. Sanz-Andrés, Bearing friction effect on cup anemometer performance modelling, in: 10th International Conference on Mathematical Modeling in Physical Sciences. September 6-9, 2021, 2021: pp. 1–8.